



# Martensitic transformation and shape memory recovery property of $\text{Cu}_{72}\text{Al}_{26.5}\text{Nb}_{1.5}$ high temperature shape memory alloy

C. Liu<sup>a,b,\*</sup>, H.W. Mu<sup>a</sup>

<sup>a</sup> School of Electronic Science, Northeast Petroleum University, Daqing 163318, China

<sup>b</sup> School of Materials Science and Engineering, Harbin Institute of Technology, Harbin 150001, China

## ARTICLE INFO

### Article history:

Received 29 March 2010

Received in revised form 17 August 2010

Accepted 24 August 2010

Available online 18 September 2010

### Keywords:

$\text{Cu}_{72}\text{Al}_{26.5}\text{Nb}_{1.5}$  alloy

Transformation behavior

Shape memory effect

Aging treatment

## ABSTRACT

Martensitic transformation and shape memory recovery property of  $\text{Cu}_{72}\text{Al}_{26.5}\text{Nb}_{1.5}$  alloy have been systematically investigated by means of differential scanning calorimeter, X-ray diffraction, transmission electronic microscopy and bending test in this work. The results show that the alloy undergoes one-step martensitic transformation from the monoclinic  $\beta_1'$  to  $\text{DO}_3$  cubic structure during the process of cooling and heating, and the martensitic transformation starting temperature of the alloy is up to 560 K, indicating the potential application in high temperature environment. TEM observations reveal that the martensites exhibit typical spear-like, plate-like and fork-like morphologies, and most of the martensite variants show self-accommodated state with (0018) twin relationship. Two kinds of the substructures of martensites are determined to be (1210) twin and (110) stacking faults for the alloy. Bending tests indicate that the aging time has remarkable influence on the shape recovery ratio of the alloy. The shape recovery ratio firstly decreases and then becomes stable with the aging duration increasing.

© 2010 Elsevier B.V. All rights reserved.

## 1. Introduction

Shape memory alloys are metallic compounds that exhibit peculiar shape memory effect and pseudoelasticity, which are related to the thermo-elastic martensitic transformation and reverse transformation [1]. Both effects can be effectively used in sensor/actuator devices. Recently, a great effort has been devoted to the shape memory alloys that can possess martensitic transformation starting temperature ( $M_s$ ) higher than 400 K [2–4]. Cu–Al–Nb alloys are newly developed high temperature shape memory alloys with the  $M_s$  temperature as high as 473 K, making them very suitable for the application in high temperature environments [5–7]. As well known, Cu-based shape memory alloys aged in different states show various behaviors and have low thermal stability, both of which are essential for the applications [8,9]. More recently, some results concerned about the effect of Nb content on microstructure and shape memory effect have been reported [10,11], however, little work has been devoted to the effect of aging time on shape recovery characteristics. The purpose of this paper is to investigate the martensitic transformation behavior of the  $\text{Cu}_{72}\text{Al}_{26.5}\text{Nb}_{1.5}$  alloy and the influence of the aging treatment on shape recovery properties.

## 2. Experimental

Alloy ingots with the mean chemical composition  $\text{Cu}_{72}\text{Al}_{26.5}\text{Nb}_{1.5}$  were prepared from pure Cu, Al and Nb of 99.99% purity by consumable arc-melting under the argon atmosphere in a water cooled copper crucible. The ingots were remelted for five times and homogenized at 1173 K for 12 h to achieve composition homogenization, followed by ice salt-water quenching. Then the ingots were hot-rolled into plates with a thickness of 2 mm at 1123 K. After that, the plates were solution treated at 1173 K for 30 min in a quartz tube with a vacuum of  $10^{-4}$  Torr and then quenched into the ice salt-water in order to remove the interference of residual strain.

The compositions of the hot-rolled alloys solution treated at 1173 K for 30 min were determined by electron probe micro-analyzer (EPMA, JXA-733) operating at 20 kV and 100 nA. Phase transformation temperature measurements for these alloys were carried out by using the differential scanning calorimeter (DSC) (Perkins-Elmer DSC-7 type) with the heating/cooling rate of 15 K/min in the temperature range from 373 to 723 K. In order to avoid oxidation at high temperature, DSC measurements were carried out in the argon gas atmosphere. The transformation temperatures were defined as the points where the peaks started to deviate from the baseline. The crystallographic structures of the hot-rolled alloys solution treated at 1173 K for 30 min were analyzed by X-ray diffraction (XRD) at different temperatures. The microstructures of these alloys solution treated at 1173 K for 30 min were observed by transmission electron microscopy (TEM) (Philips CM12 TEM/STEM, 120 kV). The foils for TEM observations were prepared by using twin-jet electro-polishing with an electrolyte of nitric acid and methanol, 1:2 in volume, at around 233 K. Shape memory effect (SME) was measured by bending test at various temperatures, as shown in Fig. 1. The pre-strain,  $\varepsilon_t = h/(d+h)$ , is about 2% in the present study. The shape recovery ratio ( $\eta$ ) was calculated in the terms of  $\eta = (\theta_d - \theta_h)/\theta_d \times 100\%$ . The temperature range for bending test was controlled by a resistor furnace with the temperature accuracy of 0.5 K. The specimens for SME measurements were cut from the hot-rolled plates along the rolling direction by spark-cut method into a dimension of  $55 \text{ mm} \times 1 \text{ mm} \times 0.4 \text{ mm}$ . These specimens were solution treated at 1173 K for 1 h in a quartz tube with a vacuum of  $10^{-4}$  Torr, and then aged at 573 and 673 K for different durations.

\* Corresponding author at: School of Electronic Science, Northeast Petroleum University, Daqing 163318, China. Tel.: +86 459 6507716; fax: +86 459 6507716.

E-mail address: [elscience@gmail.com](mailto:elscience@gmail.com) (C. Liu).

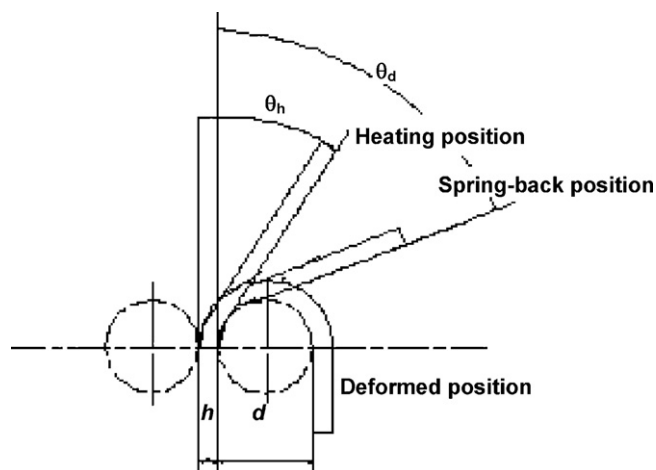


Fig. 1. Schematic illustration of the SME measurement in the bending test.

### 3. Results and discussion

#### 3.1. Martensitic transformation

DSC curve of the  $\text{Cu}_{72}\text{Al}_{26.5}\text{Nb}_{1.5}$  alloy solution treated at 1173 K for 30 min is shown in Fig. 2. The exothermic peak on the DSC cooling curve indicates that the forward martensitic transformation from austenite to martensite occurs, and the  $M_s$  temperature is approximately 560 K. The endothermic peak on the DSC heating curve is associated with the reverse martensitic transformation, where reverse martensitic transformation starting temperature ( $A_s$ ) and finishing temperature ( $A_f$ ) are 585 and 632 K, respectively. The forward and reverse martensitic transformations exhibit a typical thermo-elastic feature with a narrow temperature hysteresis ( $A_s-M_s$ ) of 25 K. Consequently, one can know that the  $\text{Cu}_{72}\text{Al}_{26.5}\text{Nb}_{1.5}$  alloy is in martensite state at room temperature. Moreover, the transformation characteristics of the  $\text{Cu}_{72}\text{Al}_{26.5}\text{Nb}_{1.5}$  alloy coincides with that of the first type thermal transformation described by Wayman [12] because of  $A_f > A_s > M_s > M_f$ .

Fig. 3 presents XRD patterns of the  $\text{Cu}_{72}\text{Al}_{26.5}\text{Nb}_{1.5}$  alloy at various temperatures. It is found from Fig. 3(a) that the crystallographic structure of the alloy at room temperature (lower than  $M_f$ ) can be identified as monoclinic  $\beta'_1$  martensitic structure. In terms of  $(\bar{1}22)$ ,  $(0018)$ ,  $(208)$  and  $(040)$  martensitic reflections, the lattice parameters of the martensitic structure are  $a=0.440$  nm,  $b=0.523$  nm,

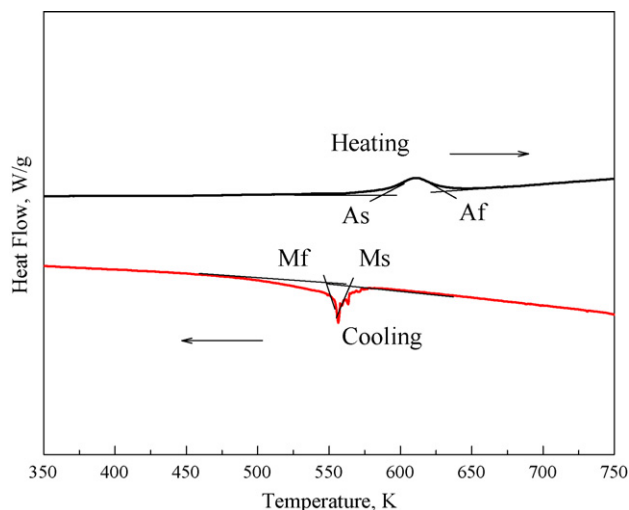


Fig. 2. DSC curve of the  $\text{Cu}_{72}\text{Al}_{26.5}\text{Nb}_{1.5}$  alloy annealed at 1173 K for 30 min.

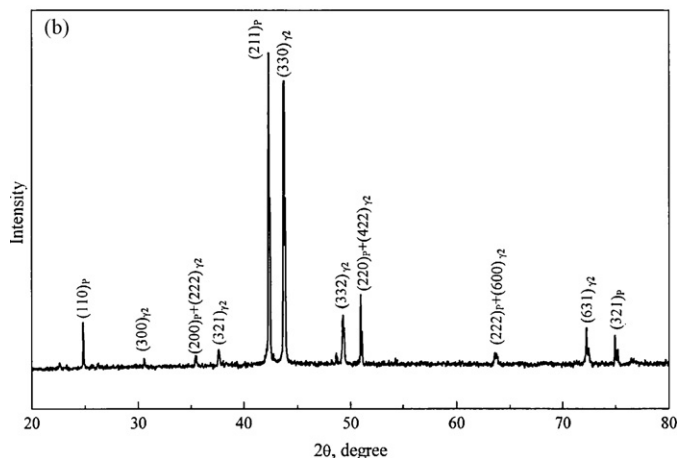
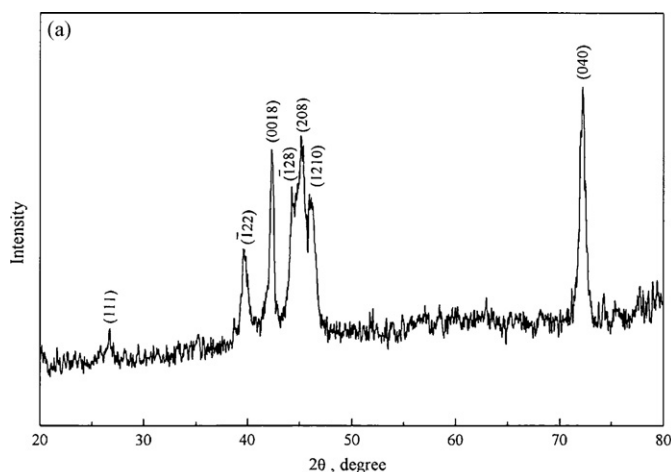


Fig. 3. XRD patterns of the  $\text{Cu}_{72}\text{Al}_{26.5}\text{Nb}_{1.5}$  alloy at various temperatures: (a) at room temperature; (b) at 723 K.

$c=3.845$  nm,  $\beta=89.45^\circ$ . The profile of this diffractogram is quite similar to that of molten Cu–Al–Ni SMA reported by Zhang et al. [13]. The XRD pattern of the alloy at 723 K ( $>A_f$ ) is indexed in Fig. 3(b) and identified as  $\text{DO}_3$  cubic austenitic structure with the lattice parameter of  $a=0.507$  nm. It is also found from Fig. 3(b) that many extra peaks are observed in the XRD pattern, which is attributed to  $\text{Cu}_9\text{Al}_4$  ( $\gamma_2$ ) precipitate.

Fig. 4 shows the transmission electron microscopy (TEM) image and select-area electron diffraction (SAED) pattern of the  $\text{Cu}_{72}\text{Al}_{26.5}\text{Nb}_{1.5}$  alloy. It is seen from Fig. 4(a) that the microstructure of the alloy mainly consists of spear-like martensites and displays typical self-accommodated morphology which is usually observed in the shape memory alloys undergoing thermo-elastic transformation. It is also found from the SAED pattern that the martensite variants are internally twinned structure, and the relationship between martensite variants is determined to be  $(0018)$  twin in terms of the indexed SAED pattern. Fig. 5 presents the TEM bright-field image and corresponding SAED pattern of the martensite in another area for the specimen. It is clearly seen from Fig. 5(a) that the boundaries of martensite variants are clear and straight. It is also found that two sets of electron diffraction patterns can be obtained in Fig. 5(b), revealing that the substructure of martensite variants is  $(1210)_M$  type I twins. In addition to twin substructure found in the  $\text{Cu}_{72}\text{Al}_{26.5}\text{Nb}_{1.5}$  alloy, stacking faults are observed by TEM in this alloy as shown in Fig. 6. It is seen from Fig. 6(a) that the studied martensitic domains consist of fine and dense stacking strips with different orientations. It is also worthy of noting that the angle of these strips and the martensite interface is

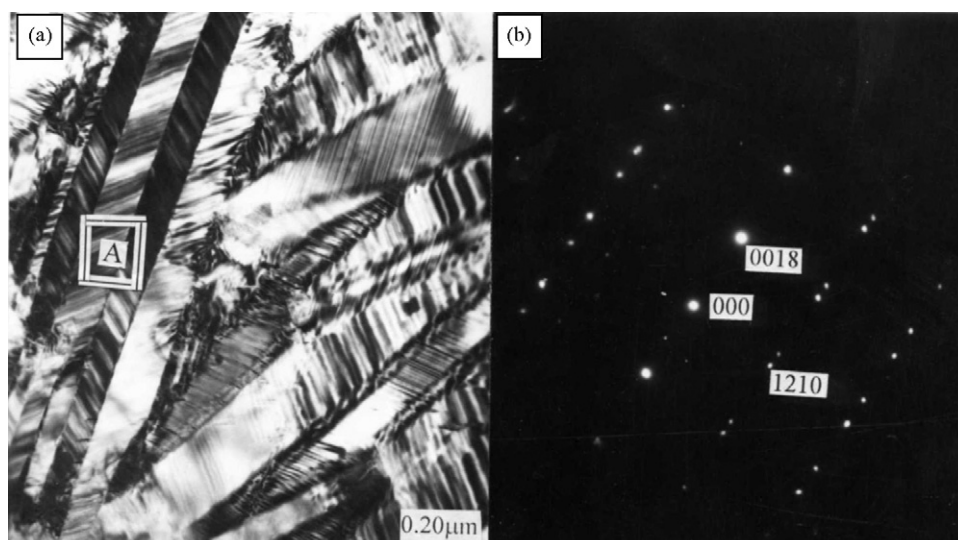


Fig. 4. The transmission electron microscopy (TEM) image and select-area electron diffraction (SAED) pattern of the  $\text{Cu}_{72}\text{Al}_{26.5}\text{Nb}_{1.5}$  alloy.

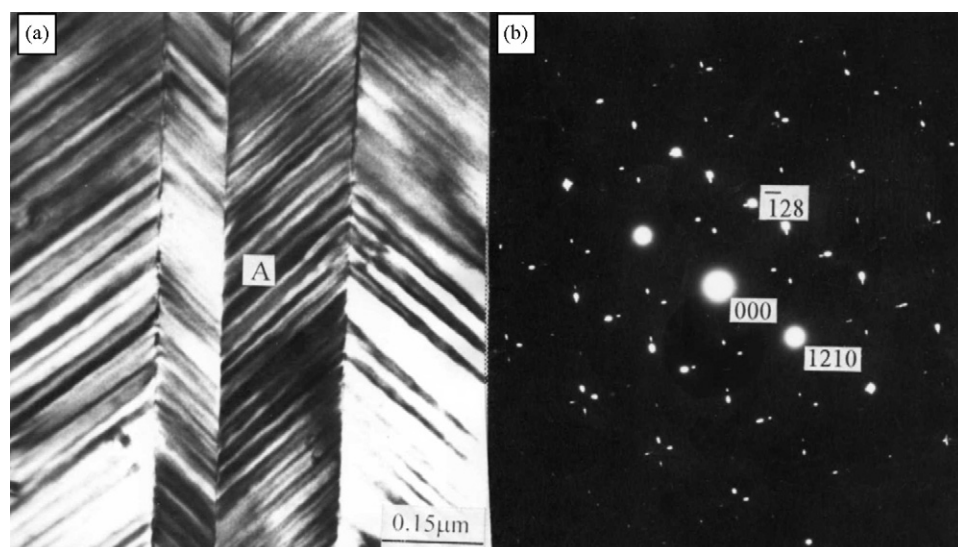


Fig. 5. TEM image (a) and SAED pattern (b) taken from the inner of variants for  $\text{Cu}_{72}\text{Al}_{26.5}\text{Nb}_{1.5}$  alloy.

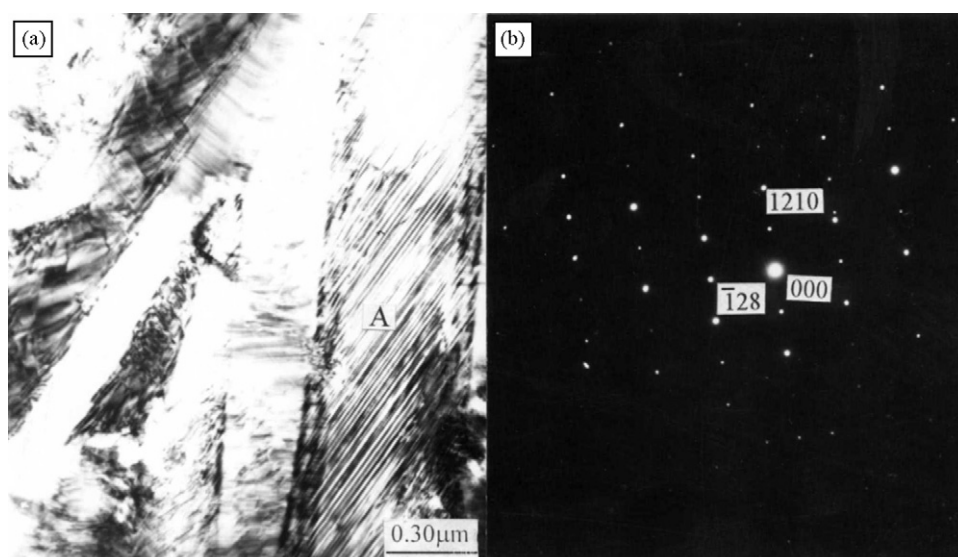


Fig. 6. TEM image and SAED pattern showing the (110) stack fault for the  $\text{Cu}_{72}\text{Al}_{26.5}\text{Nb}_{1.5}$  alloy.

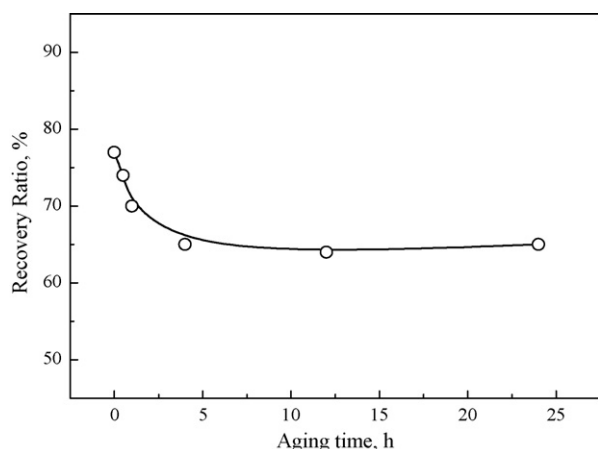


Fig. 7. Effect of the aging time on the shape recovery ratio of the  $\text{Cu}_{72}\text{Al}_{26.5}\text{Nb}_{1.5}$  alloy aged at 573 K.

approximate  $45^\circ$ , and these paralleled strips transverse the whole martensite. Accordingly, it is obtained from Fig. 6(b) that the substructure of the martensite variants observed in this region is (1 1 0) stacking faults.

### 3.2. Shape recovery

Fig. 7 shows the shape recovery ratio of the  $\text{Cu}_{72}\text{Al}_{26.5}\text{Nb}_{1.5}$  alloy specimens quenched from 1173 K and aged at 573 K as a function of the aging time. It is seen that the shape recovery ratio of the  $\text{Cu}_{72}\text{Al}_{26.5}\text{Nb}_{1.5}$  alloy can be divided into two stages. At the first stage of aging treatment, the shape recovery ratio decreases dramatically when the aging time increases up to 5 h, and then becomes stable as the aging time further increases to 24 h. So it is reasonable to believe that the reverse martensitic transformation is suppressed by the aging treatment, termed “stabilization of martensite” [14]. This phenomenon can be attributed to the pinning effect of the interfaces between the parent phase and martensite phase as well as the interfaces between martensite variants induced by the concentration of the quenched-in vacancies occurring in aging treatment.

Fig. 8 shows the dependence of shape recovery ratio on the aging time of the  $\text{Cu}_{72}\text{Al}_{26.5}\text{Nb}_{1.5}$  alloy specimens aged at 673 K for a series of time duration 0.5–24 h. It is clearly seen that the shape recovery ratio of the alloy aged in parent state presents the same behavior as the sample aged in martensite state. The shape recovery ratio decreases with increasing the aging time in the early stage and then achieves a constant value when the aging time exceeds 4 h. It is also found that fracture occurs during bending tests when the alloy is aged up to 24 h. The phenomena above mentioned are mainly related to  $\gamma_2$  phase precipitating when the alloy is aged in austenite state. It is explained that  $\gamma_2$  phase is brittle and cannot possess thermo-elastic martensitic transformation behavior, leading to the decrease of thermo-elastic martensite variants during reverse martensitic transformation. In addition,  $\gamma_2$  phase precipitating at grain boundary can form a network structure in the alloy, resulting in the decrease of the fracture strength.

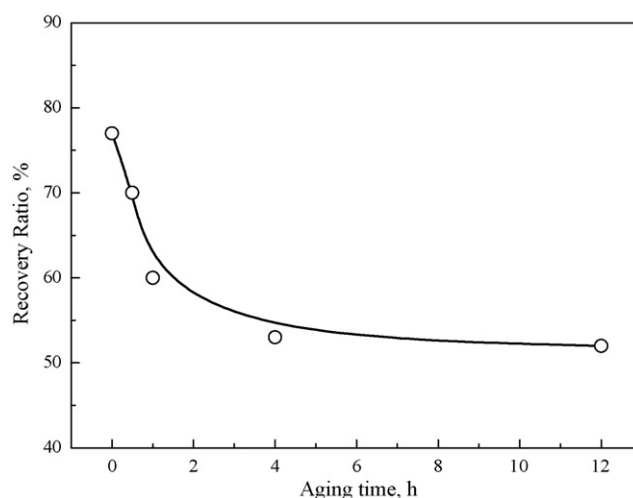


Fig. 8. Effect of the aging time on the shape recovery ratio of the  $\text{Cu}_{72}\text{Al}_{26.5}\text{Nb}_{1.5}$  alloy aged at 673 K.

## 4. Conclusions

The  $\text{Cu}_{72}\text{Al}_{26.5}\text{Nb}_{1.5}$  alloy undergoes one-step thermo-elastic martensitic transformation behavior during the process of heating and cooling. The  $\gamma_2$  phase precipitates in the austenite matrix.

The martensite variants show self-accommodated morphology with (00 1 8) twin relationship. (1 2 1 0) twin and (1 1 0) stacking faults substructures are found in the martensites.

The shape recovery ratio of the alloy aged in both martensite and austenite state decreases with the aging time increasing in the early stage and then becomes stable.

## Acknowledgment

This work has been supported by the Foundation of Heilongjiang Province for Returned Scholars (Granted No. LC2009C11).

## References

- [1] C.M. Wayman, K. Shimizu, *Met. Sci.* 6 (1972) 175–183.
- [2] J.V. Humbeeck, *Trans. ASME* 121 (1999) 98–101.
- [3] J.V. Humbeeck, *Mater. Sci. Eng. A* 273–275 (1999) 134–148.
- [4] C.H. Man, C.Y. Chung, *Mater. Sci. Forum* 327–328 (2000) 497–500.
- [5] J. Leltko, H. Morawiec, Y.N. Koval, V.I. Kolomytsev, *Inżynieria Materialowa* 3 (1998) 471–474.
- [6] S.K. Gong, Y.Q. Ma, C.B. Jiang, H.B. Xu, *Mater. Sci. Forum* 394–395 (2002) 383–386.
- [7] J. Leltko, H. Morawiec, M. Gigla, Y.N. Koval, V.I. Kolomytsev, *Applied Crystallography: Proceedings of the XVII Conference, Wisla, Poland, 1997*, p. 312.
- [8] M. Gigla, J. Leltko, H. Morawiec, *Proceedings of Conference on Electron Microscopy of Solids, Serock, Poland, 1999*, p. 231.
- [9] T. Tadaki, M. Takamwri, K. Shmizu, *Mater. Trans. JIM* 28 (2) (1987) 120–128.
- [10] K. Otsuka, X. Ren, *Mater. Sci. Eng.* 312 (2001) 207–218.
- [11] H. Morawiec, J. Leltko, Y.N. Koval, V.I. Kolomytsev, *Mater. Sci. Forum* 327–328 (2000) 291–294.
- [12] C.M. Wayman, *Suppl. Trans. JIM* 17 (1976) 159–170.
- [13] Y.M. Zhang, J.N. Gui, R.H. Wang, L.M. Gao, Y.M. Wu, Y.L. Thang, *J. Phys. Condens. Matter* 5 (1993) 2719–2728.
- [14] Z.Y. Gao, Y. Wu, Y.X. Tong, W. Cai, Y.F. Zheng, L.C. Zhao, *J. Mater. Sci.* 41 (2006) 6165–6167.